

Study of the Depolarized Light Scattering Spectra of Supercooled Liquids by a Simple Mode-Coupling Model

V.Krakoviack*, C.Alba-Simionescu†, M.Krauzman

CPMA[‡], bâtiment 490, université Paris-Sud, F-91405 Orsay, France

Abstract

By using simple mode coupling equations, we investigate the depolarized light scattering spectra of two so-called "fragile" glassforming liquids, salol (phenylsalicylate) and CKN ($\text{Ca}_{0.4}\text{K}_{0.6}(\text{NO}_3)_{1.4}$), measured by Cummins and coworkers. Nonlinear integrodifferential equations for the time evolution of the density-fluctuations autocorrelation functions are the basic input of the mode coupling theory. Restricting ourselves to a small set of such equations, we fit the numerical solution to the experimental spectra. It leads to a good agreement between model and experiment, which allows us to determine how a real system explores the parameter space of the model, but it also leads to unrealistic effective vertices in a temperature range where the theory makes critical asymptotic predictions. We finally discuss the relevance and the range of validity of these universal asymptotic predictions when applied to experimental data on supercooled liquids.

*e-mail : krako@cpma.u-psud.fr

†e-mail : chalba@cpma.u-psud.fr

‡fax-number : (33/0) 1.69.15.42.00

1 Introduction

Understanding the properties of the supercooled liquids is still a challenging problem. This explains the considerable amount of work on the subject from the experimental as well as from the theoretical point of view. Of great interest is the fact that, whereas the static properties of a supercooled liquid vary weakly in the temperature range between the melting temperature T_m and the so-called calorimetric glass transition temperature T_g , the dynamical properties such as transport coefficients exhibit a strong temperature dependence. In particular, for 'fragile' liquids (according to Angell's classification¹), the viscosity shows a strongly non arrhenian behavior : it increases slowly with decreasing temperature in the weakly supercooled domain (near T_m), but changes by many orders of magnitude when approaching T_g . Below this point, the systems falls out of metastable equilibrium and becomes a non ergodic amorphous solid, the glass. Such an observation leads to assume the existence of two dynamical regimes crossing over at a certain temperature.

From this experimental background, the mode coupling theory (MCT)² proposes a mechanism for the dynamics of supercooled liquids based on density fluctuations : a closed set of integrodifferential equations is established within the formalism of the generalized Langevin equation by approximating the memory function as polynomials of density correlators; a bifurcation scenario is then elaborated and describes the liquid-glass transition as one from an ergodic liquid state with zero Debye-Waller factor (DWF) to a non-ergodic ideal glassy state with non-zero DWF. A dynamical critical transition at which the singularity is expected to occur is then introduced at a temperature T_c higher than T_g . Due to its critical nature the MCT makes a number of universal predictions in the vicinity of T_c . In particular, the q -dependence of the density correlators should vanish in the intermediate-time or -frequency domains where two relaxations, α and β , overlap, the dynamics being described by a single function only depending on a unique parameter λ . A square-root singularity of the DWF and a power-law divergence of the viscosity are predicted too.

To date most comparisons of the MCT to experimental data rely on these predicted universal features, although the range of validity of the approximations leading to these predictions is not well determined (only recently, the necessary corrections to these asymptotic predictions have been investigated for hard spheres³). A different approach is to choose a reduced set of mode-coupling equations (then called "schematic equations") and to fit its full solution to experimental data with no direct reference to the expected critical properties.⁴ Such a method, although very simplified, has the advantage of taking explicitly into account the microscopic dynamics, which is impossible by other means, and of allowing an assessment of the range of validity of the universal predictions. A restricted study has already been presented for the Raman spectra of several molecular glassformers (*m*-toluidine and other disubstituted benzenes, glycerol) in the frequency range from 150 GHz to 6000 GHz.^{4,5}

In this paper, we propose to apply this method to a wider frequency range⁶ in order to fit the depolarized light scattering (DLS) spectra of salol (an aromatic molecular liquid) and CKN (a binary molten salt) between 0.3 GHz and 5000 GHz, as measured by Cummins and coworkers. Many different experimental techniques have been applied to them, allowing tests of many aspects of the theory. A summary of these experimental results is proposed for comparison with our results in table 1 for salol and table 2 for CKN. In the next section, we briefly describe the experimental support and some spectral features that our model has to take into account. In section 3, we review theoretical results needed for data analysis and discussion. Our model and data processing are presented in section 4, whereas fitting results are exposed in section 5. A discussion of the MCT predictions is given in section 6 and conclusions appear in section 7.

2 Experimental support and spectral trends

We have analyzed the VH light scattering spectra of supercooled salol

and CKN obtained by Cummins and coworkers by combining both Raman and Brillouin scattering in the frequency range between 0.3 GHz and 5000 GHz. The temperatures of experimentation cover the whole domain of the supercooled liquid state, from just above the melting point to the calorimetric glass transition. These spectra have been already extensively studied in the context of the universal predictions of the MCT (^{7,8} for salol, ^{8,12} for CKN) and the reader is referred to these articles for experimental details.

Rather than the experimental scattered intensity, the susceptibility spectra are more suited for a comparison with MCT predictions. These are obtained by normalizing the experimental intensities by the Bose factor :

$$\chi''(\omega) = \frac{I^{exp}(\omega)}{n(\omega) + 1} \quad \text{with} \quad n(\omega) = \frac{1}{\exp(\frac{\hbar\omega}{k_B T}) - 1}. \quad (2.1)$$

In the following, the term spectra will always refer to this frequency-dependent susceptibility.

The spectra of salol present some general features shared by many aromatic fragile supercooled liquids of the same kind like *o*-terphenyl,^{17,18} *m*-toluidine,⁴ *m*-cresol and others.⁵ These are :

- a double high-frequency peak with principal frequency at about 3600 GHz and a shoulder at 600 GHz, often referred to as ‘Boson’ peak and whose physical interpretation is not yet definitive.^{5,18–21} This part of the spectra is almost temperature-independent and is assigned to microscopic excitations of the system.
- a low frequency peak which maximum frequency decreases rapidly with temperature according to a non arrhenian law. It corresponds to the α -relaxation processes.
- the intensity of the α -peak is a lot greater than that of the microscopic band.
- the shape of the α -peak is characteristic of a stretched, rather than exponential, relaxation.

- a minimum occurs between these two structures with an enhancement of intensity at higher frequencies due to the so-called fast β -relaxation : this region, where α - and β -relaxations cross, is the domain of interest to test the universal predictions made by the MCT.

The spectra of CKN, a fragile ionic glassformer, exhibit the same features except for two points :

- the height of the α -peak is much lower, *i.e.* it has roughly the same intensity as the microscopic band.
- no pronounced extra-structure is distinguishable in the microscopic region.

These differences may originate from the fact that both the translational and rotational molecular motions are detected, as suggested first for the *o*-terphenyl spectra.¹⁷ Indeed, the nature of the process that dominates VH spectra, interaction-induced or reorientation-induced scattering, has been investigated for the different parts of the spectra of salol.²² It was found that below the microscopic band the second mechanism is dominant, while a constant depolarization ratio of 0.75 was measured for all these liquids above 600 GHz, supporting a dipole-induced dipole (DID) mechanism. Therefore, the observed differences could be simply related to a different weighting of these two contributions. This problem will be further discussed in section 5.

3 Mode-coupling theory of the glass transition

As a starting point, the Mode Coupling Theory of the liquid-glass transition assumes that the dynamics of a supercooled liquid is entirely governed by the density fluctuations and proposes a set of generalized kinetic equations (*à la* Mori-Zwanzig) for the normalized autocorrelation functions $\phi_q(t)$

of the density fluctuations modes at wave vector q , $\rho_q(t)$.² These equations take the form :

$$\ddot{\phi}_q(t) + \Omega_q^2 \phi_q(t) + \int_0^t M_q(t-t') \dot{\phi}_q(t') dt' = 0, \quad (3.1)$$

where the memory kernel is split into an instantaneous damping term $\gamma_q \delta(t)$ and a mode-coupling term $m_q(t)$:

$$M_q(t) = \Omega_q^2 [\gamma_q \delta(t) + m_q(t)]. \quad (3.2)$$

The core of the mode coupling approximation in the "idealized case" only considered here is to express $m_q(t)$ as a polynomial function F_q of the $\phi_q(t)$'s, so that

$$m_q(t) = F_q(\mathbf{V}, \phi_k(t)) = \sum_{n \geq 1} \sum_{q_1, \dots, q_n} V_{q_1, \dots, q_n} \phi_{q_1}(t) \dots \phi_{q_n}(t), \quad (3.3)$$

where the components of the vector \mathbf{V} , the vertices V_{q_1, \dots, q_n} , are positive continuous functions of the static structure factor $S(q)$. It should be noticed that the linear terms in $m_q(t)$ are introduced in an *ad hoc* fashion to guarantee that models with only a very reduced set of equations reproduce the stretched behavior of the α -relaxation. Some justifications of the presence of these terms have been proposed in the context of the non-linear fluctuating hydrodynamics.²³ The mode-coupling equations are finally written as :

$$\ddot{\phi}_q(t) + \gamma_q \Omega_q^2 \dot{\phi}_q(t) + \Omega_q^2 \phi_q(t) + \Omega_q^2 \int_0^t m_q(t-t') \dot{\phi}_q(t') dt' = 0, \quad (3.4)$$

with $m_q(t)$ given by equation 3.3.

This set of equations can lead to an ergodic-to-non ergodic transition. Indeed, the Debye-Waller factors (DWF) defined by

$$f_q = \lim_{t \rightarrow +\infty} \phi_q(t) \quad (3.5)$$

are solutions of the set of equations :

$$\frac{f_q}{1 - f_q} = F_q(\mathbf{V}, f_k). \quad (3.6)$$

The only real solution in the vicinity of $\mathbf{V} = 0$ is the trivial one (for all q 's, $f_q = 0$) corresponding to an ergodic liquid state. A bifurcation to a non zero solution corresponding to a non ergodic "ideal glassy state" occurs when a critical hypersurface, the "ideal glass transition hypersurface", is crossed. It is defined by a vector \mathbf{V}^c such that the Jacobian matrix of equations 3.6 is singular, so that :

$$\frac{f_q^c}{1 - f_q^c} = F_q(\mathbf{V}^c, f_k^c) \quad (3.7)$$

$$\det \left[\frac{1}{(1 - f_q^c)^2} \delta_{qp} - \frac{\partial F_q}{\partial f_p}(\mathbf{V}^c, f_k^c) \right] = 0. \quad (3.8)$$

Two type of transitions exists : the A-type with the DWF varying continuously through the transition hypersurface and the B-type with discontinuous change of the DWF. The second one is the only potentially relevant in the context of the liquid-glass transition. At the thermodynamic level, intensive critical parameters (critical temperature, density and so on), at which the transition is supposed to occur, are defined.

In the vicinity of the transition hypersurface, it is possible to make various predictions on the critical behavior of the solutions of the mode coupling equations, the most important being the "reduction theorem". Expanding to lowest order in $\mathbf{V} - \mathbf{V}^c$, one obtains

$$\phi_q = f_q^c + (1 - f_q^c)^2 G_q(t), \quad (3.9)$$

where the leading contribution to G_q , in the vicinity of the plateau of ϕ_q , is proportional to a q -independent function G , which is solution of the equation (called the scaling equation)

$$\sigma + \lambda G(t)^2 - \frac{d}{dt} \int_0^t G(t - t') G(t') dt' = 0, \quad (3.10)$$

where σ , the separation parameter, is an $O(\mathbf{V} - \mathbf{V}^c)$ given by

$$\sigma = \sum_q \hat{e}_q \left(F_q(\mathbf{V}, f_k^c) - \frac{f_q^c}{1 - f_q^c} \right) \quad (3.11)$$

and is positive in the ideal glassy state, negative in the liquid, and zero on the transition hypersurface. The exponent parameter λ is defined by

$$\lambda = \frac{1}{2} \sum_{q,k,p} \hat{e}_q \left(\frac{\partial^2 F_q}{\partial f_k \partial f_p}(\mathbf{V}^c, f_l^c) \right) (1 - f_k^c)^2 (1 - f_p^c)^2 e_k e_p, \quad (3.12)$$

with $[e_q]$ and $[\hat{e}_q]$ eigenvectors of the matrix 3.8.²

Eqs. 3.9 and 3.10 and some of their consequences have been extensively used to test the validity of MCT by comparison with experimental data. In particular, an approximate expression around the susceptibility minimum has been proposed :

$$\chi''(\omega) = \frac{\chi''_{min}}{a+b} \left(b \left(\frac{\omega}{\omega_{min}} \right)^a + a \left(\frac{\omega_{min}}{\omega} \right)^b \right), \quad (3.13)$$

with a and b such that

$$\lambda = \frac{\Gamma(1-a)^2}{\Gamma(1-2a)} = \frac{\Gamma(1+b)^2}{\Gamma(1+2b)}. \quad (3.14)$$

The relevance of such studies will be discussed in section 6.

4 Model and data processing

In our calculations, we intend to take into account the properties of the spectra in the THz domain such as the microscopic peak and the inelastic boson peak. This is not possible with studies by means of the scaling equation, eq. 3.10 or eq. 3.13, because they are restricted to the region around the minimum of the susceptibility spectrum, *i.e.* to the GHz domain. Thus, we choose to study in full detail a schematic model, *i.e.* a restricted set of mode-coupling equations like eq. 3.4 with a simple form of the memory functions, eq. 3.3.

The basis of our study is the well-studied F_{12} -model² for a single correlator ϕ_0 defined by

$$\ddot{\phi}_0(t) + \Gamma_0 \Omega_0 \dot{\phi}_0(t) + \Omega_0^2 \phi_0(t) + \Omega_0^2 \int_0^t m_0(t-t') \dot{\phi}_0(t') dt' = 0, \quad (4.1)$$

$$m_0(t) = v_1 \phi_0(t) + v_2 \phi_0^2(t). \quad (4.2)$$

We add a second correlator ϕ_1 in order to reproduce the double-hump shape of the peak in the THz domain and the extra-intensity of the α -peak. It is solution of

$$\ddot{\phi}_1(t) + \Gamma_1 \Omega_1 \dot{\phi}_1(t) + \Omega_1^2 \phi_1(t) + \Omega_1^2 \int_0^t m_1(t-t') \dot{\phi}_1(t') dt' = 0. \quad (4.3)$$

It remains to express the memory kernel m_1 . For this purpose, we take the first correlator ϕ_0 accounting in an effective way for all modes that are responsible for the underlying critical transition (typically, these are thought to be the density fluctuations at wave vectors corresponding to the maximum of the static structure factor²⁴). The second correlator ϕ_1 describes additional degrees of freedom, that are important in depolarized light scattering processes but whose slow time-dependence is dominated by that of ϕ_0 (so that the liquid-glass transition occurs systematically for the two correlators at the same time). A simple choice is then

$$m_1(t) = r m_0(t). \quad (4.4)$$

In addition we impose that the characteristic pulsations (Ω_0, Ω_1), the damping coefficients (Γ_0, Γ_1) and the coupling parameter r are temperature-independent. As a consequence, the whole temperature dependence is contained in the vertices v_1 and v_2 .

The above model has a B-type transition, and the critical hypersurface reduces to a line in the 2-dimensional parameter space (v_1, v_2) :

$$v_1^c = 2\sqrt{v_2^c} - v_2^c \quad \text{with} \quad 1 \leq v_2^c \leq 4 \quad (4.5)$$

The exponent parameter is :

$$\lambda = \frac{1}{\sqrt{v_2^c}}. \quad (4.6)$$

Other models with two correlators have already been proposed in a similar context : the Sjögren model for diffusion of impurities in a glass-forming liquid²⁵ and the Bosse-Krieger model for coupled mass-density and charge-density correlators in a supercooled molten salt.²⁶

It should be noted that, because of the extreme simplicity of the model, the real nature of the correlators is somewhat obscured. ϕ_0 and ϕ_1 are not necessarily restricted to be density correlators. In particular, the model could account for molecular orientational fluctuations or any other degrees of freedom that are not included in standard MCT. Accordingly, the parameters that we extract from the fits do not have a precise microscopic content and should be considered as a minimal set of phenomenological quantities that allows to describe the global evolution of the systems in the context of simple mode-coupling models.

To compare the predictions of the model to the experimental data, it is also necessary to make some assumptions about the mechanism that gives rise to the light scattering spectra. When the dipole-induced dipole (DID) mechanism dominates, as often assumed,^{8,27} the Stephen factorization scheme²⁸ (which is compatible with the factorization approximations underlying the MCT) leads to an expression for the DLS spectrum $\chi''(\omega)$ which involves the Fourier transform of bilinear products of the correlators. A simple description of the spectrum for the case of our two-correlator model is similarly given by :

$$\chi''(\omega) = \omega A \operatorname{Im} \left\{ \operatorname{FT} \left[\phi_0(t)^2 + \gamma \phi_1(t)^2 \right] \right\} \quad (4.7)$$

with FT denoting Fourier transform and Im the imaginary part. A is an amplitude factor that we take dependent of temperature. γ is an *ad hoc* parameter which specifies the relative weight of the two contributions to the DLS spectrum due to ϕ_0 and to ϕ_1 and which we take as temperature independent. However, both A and γ are substance-dependent. This expression of the scattered intensity corresponds to the assumption that ϕ_0 and ϕ_1 are both density correlators. Nevertheless, as pointed in ref. 22, fluctuations of the molecular orientations are a major contribution to the DLS spectra. In order to test the dependence of our results in the chosen expression of the scattered intensity, we have also performed tests with other choices for the expression of the susceptibility $\chi''(\omega)$, like a linear combination of the correlators or 'mixed' models, quadratic in ϕ_0 and linear in ϕ_1 .²⁹ The fits

were not as good as with eq. 4.7 in the microscopic part of the spectra, but they were equivalent in the region of the minimum of susceptibility and of the α -peak. The values of the vertices and of other parameters of the model *were only very weakly affected by the modification*. It seems thus that the question of the nature of the light scattering mechanisms is not determining for our study. It remains out of our scope.

The calculations consist of three steps :

- 1) the time evolution of the correlators ϕ_0 and ϕ_1 is computed from equations 4.1 to 4.4 by means of an algorithm derived from the one described in reference³⁰ and provided to us by M.Fuchs and W.Götze.
- 2) The Fourier transform in equation 4.7 is performed via the Filon algorithm³¹ to obtain theoretical susceptibilities $\chi''(\omega)$.
- 3) The preceding calculations are included in a loop using a modified least-square Powell algorithm³² where the T -dependent parameters A, v_1 and v_2 and the T -independent parameters $\Omega_0, \Omega_1, \Gamma_0, \Gamma_1, r$ and γ are adjusted to provide the best fit between model and experiment.

Analogous calculations have been performed for different choices of the polynomial approximation to the memory function m_0 to fit Raman scattering spectra of m -toluidine.⁴ Good and stable fits were obtained with the F_{12} -model associated with equation 4.7 for $\chi''(\omega)$, so we restrict mostly ourselves to this case. We have used different functional forms of the memory functions to fit the salol spectra, but the results are still preliminary and will be only briefly mentioned.²⁹

5 Numerical results

A major difficulty with the MCT in its formulation only in terms of density fluctuation modes is that it predicts the existence of a sharp ergodic-to-non ergodic transition that is not observed experimentally. This transition

which is assumed to be at a temperature T_c higher than T_g is avoided because of so-called activated processes that are not taken into account by the theory and that restore ergodicity below T_c . For this reason, the low-temperature features predicted below T_c are always obscured in the supercooled liquid state and the rare characterizations of these¹² do not come without any polemics.³³ It is thus necessary to impose some temperature limitations to the fitted data by ignoring the coldest spectra or imposing a low-frequency cut-off for the lowest temperatures in order to free our calculations from this difficulty without losing any microscopic information. It is clear that such constraints will affect the fitting results. This point is discussed later on.

Typical fits to experimental data are shown in figure 1 at different temperatures for both liquids. With the chosen cut-offs (typically about 100 GHz for temperatures below the best fit to T_c . See fig. 1.a), the schematic spectra are in very good agreement with the data. In particular, at high temperature, the whole spectra are reproduced by the model including well defined α and microscopic peaks. Thus this set of equations in the mode-coupling formalism ensures the continuity of the dynamical processes from the transient vibrational regime of the microscopic band to the regime of structural relaxation. A drastic difference of behavior exists between high and low temperatures as far as a choice of frequency cut-off is concerned. Out of the restricted fitting frequency range, a reasonable extrapolation to low frequencies is possible for high temperatures, whereas it is impossible at low temperatures. This is due to the limitations of the theory discussed above. In the first case (high T), the spectra can be described unambiguously by the model, but, in the second case (low T), the theory does not describe the α -relaxation at all and the fits force the low-temperature predictions of MCT to occur below the frequency cut-off, giving unstable and unphysical results.

The calculated temperature-independent parameters of the model are presented in table 3. The choice of frequency cut-off has little influence on these values. Error bars of about 15 % are determined from different choices. The

values obtained for the frequencies are realistic in regard to the position of the microscopic bands.

The coupling parameter r measures the strength of the coupling of the correlator ϕ_1 to the driving correlator ϕ_0 . From the fits to both salol and CKN data, it is found greater than one. This supports the assumption that processes can be isolated that drive the overall dynamics of the system.

An interesting result is that the relative weight γ of the second correlator contribution to the DLS spectra is greater than one and greater for salol than for CKN. This is illustrated in figure 2 where the two terms of equation 4.7 are considered separately. It is clear from the figure that the main contribution to the spectra is due to the second correlator ϕ_1 , except for the highest frequencies. Therefore the first correlator seems to drive the overall slowing down of the system, whereas the second one provides the experimental probe of the dynamics. It is an interesting consequence of the fitting procedure chosen with eq. 4.7 to allow such a classification. Moreover, we may assess the contribution of the second correlator depending on the chemical nature of the liquid (aromatic or ionic), at least with our specific F_{12} model. Departing from the original MCT scenario that deals only with density fluctuations and since our results are independent of the expression of the scattered intensity as a function of the correlators (see section 4), thus of their precise physical content, one could interpret this result in a way compatible with ref. 22 : orientational fluctuations represented by ϕ_1 produce the main part of the depolarized light scattering spectra and are strongly coupled to density fluctuations represented by ϕ_0 which drive the dynamics of the supercooled liquid above T_c . It would be necessary to support this assumption to demonstrate that the dynamics of the orientational and density fluctuations obey similar mode-coupling equations, which remains to be done.

We have also let r and γ vary with temperature. However, it does not produce better fits despite the considerable amount of new adjustable parameters and it was abandoned.

The most important output of our calculations are the effective-temper-

ature dependent vertices v_1 and v_2 (figures 3 and 4). Indeed, the knowledge of these parameters gives access to the way a realistic system explores the parameters space of the model (see figure 4). It thus allows to discuss the applicability of the asymptotic predictions of the theory in the vicinity of T_c . See below.

For determining the vertices, the problem of the low-frequency cut-off must be addressed, again because of the limitations of the theory discussed above. At high temperatures, the vertices are determined unambiguously, irrespective of the cut-off : whether one restricts the fitting range to the microscopic peak and its "fast- β -relaxation" wing (*i.e.* a cut-off at about 100 GHz) or includes the region of the susceptibility minimum, and considers or not the α -peak has no influence on the results. On the contrary, at low temperatures where the theory cannot apply to the full spectrum, the fitting procedure gives results that are cut-off-dependent and unstable. This produces unphysical discontinuities in the behavior of v_1 and v_2 when crossing the dynamical-transition line. With no frequency cut-off (other than the one due to the experimental frequency window), the limitations of the theory appear in a rather surprising way on the fitted values of the vertices. At the lowest temperatures, the representative curves of salol and CKN seem to follow asymptotically the transition line as the temperature is lowered (see figure 4). Implications of this observation are discussed in the next section.

Note finally that the choice for the expression of the DLS susceptibility as a function of the correlators ϕ_0 and ϕ_1 has no influence on the values of the vertices that we obtain. Linear or quadratic expressions produce undistinguishable results. This supports our analysis and conclusions, which are independent of the detailed description of the light scattering process.

6 Critical properties

Knowing how a real system explores the parameter space of the model can give some insight into the applicability of the MCT universal predictions

to experimental data. This is the purpose of our schematic model to provide such a knowledge.

As discussed in the preceding section, the "idealized" MCT used here fails in describing the dynamics of the strongly supercooled liquids, *i.e.* below the critical temperature T_c introduced by the theory itself. It is thus necessary in general to impose temperature and/or frequency limitations to the experimental data under study in order to compare with the theoretical predictions. Fortunately, this has no influence on the high-temperature results. For this reason, we consider in the following only the results obtained without explicit frequency cut-off. Doing so, the cut-off dependence of our results, a possible objection to mode-coupling tests,³³ is avoided and the comparison with other tests of the theory is made easier. The penalty is of course that one must impose a low-temperature cut-off.

The adjusted effective vertices exhibit two regimes with temperature. Above and slightly below the melting temperature, they vary linearly (v_1 is almost constant), whereas, at lower temperature, they tend to follow asymptotically the transition line without crossing it. As the static structure factor evolves only slowly with temperature in the supercooled liquid state, the rapid departure from the quasi-linear behavior appears to signal a breakdown of the usual MCT hypothesis that the vertices are continuous functions of the static correlations and vary moderately with temperature. If the critical properties are determined by extrapolation from the quasi-linear domain only (table 4), the critical temperatures T_c for salol and CKN are found in good agreement with the previous determinations (compare table 4 and tables 1 and 2). It must be noted that the corresponding critical temperatures fall in the low-temperature but still ergodic regime. An exponent parameter λ_{HT} can be determined from this high-temperature behavior. It is in good agreement with previous determinations for salol but is significantly smaller for CKN (see tables).

Other extrapolations are possible by including the nonlinear regime. Once one includes this regime, the critical temperatures and the exponent param-

eters depend on the low-temperature cut-off, and, if one wants to include more data, on low-frequency cut-offs as well. It is found that the smaller the low-temperature cut-off, the smaller the extrapolated critical temperature, and the smaller the exponent parameter λ , as can be seen in figure 4. In an extreme situation, without any frequency cut-off (and with a wider experimental frequency window), because the fitting procedure forces T_c to be smaller than all the considered temperatures, it appears that no transition could be defined at all, as the vertices follow asymptotically the transition line without crossing it. Unphysical values could then be obtained, like v_1 becoming negative.

Of particular interest is the exponent parameter extrapolated from the effective vertices at the critical temperature determined from the linear regime. It is referred to as λ_{vert} in table 4. Whereas one would expect λ_{vert} to be compatible with the previous determinations of λ based on the critical predictions of the theory (tables 1 and 2), it is found significantly smaller for both salol and CKN. This discrepancy should then affect strongly the quality of a master equation fit and limit its range of validity.

We have also proceeded with different schematic models, a F_{13} -based one with

$$m_0 = v_1 \phi_0 + v_3 \phi_0^3 \quad m_1 = r m_0 \quad (6.1)$$

and a Sjögren-like one²⁵ with

$$m_0 = v_1 \phi_0 + v_2 \phi_0^2 \quad m_1 = r \phi_0 \phi_1. \quad (6.2)$$

Results of the fitting procedure are in total agreement with the above picture.²⁹

It is interesting to relate our results to the numerical studies on binary mixtures of Lennard-Jones atoms³⁴ and soft spheres.³⁵ For both systems, the static structure factors have been used to determine the vertices of the memory kernels in the mode-coupling equations. Then, the critical properties and the long-time dynamics obtained from the equations have been compared to the molecular dynamics simulation results. It is systematically found

that this mode-coupling approach overestimates the ability of the system to freeze in an "ideal glassy state". The physical interpretation of this effect is clear : restricting the relevant dynamical modes to the density fluctuations excludes possible alternative decay channels for relaxations and the freezing occurs more rapidly. In the case of the Lennard-Jones system, the exponent parameter calculated from the mode-coupling model ($\lambda = 0.708$; for soft spheres it is $\lambda = 0.73$) is found smaller than that determined from a fit to the scaling equation ($\lambda = 0.78 \pm 0.02$). For both systems, the diffusion constant seems to vanish (at an extrapolated temperature) with a power law corresponding to $\lambda \simeq 0.60$, whereas the α -relaxation times seem to diverge with power laws corresponding to $\lambda \simeq 0.79$ for the Lennard-Jones system and $\lambda \simeq 0.88$ for the soft spheres. This is in contradiction with the requirement that a given system be characterized by a single exponent parameter λ .

These discrepancies on the value of λ are surprisingly quantitatively very similar to those found from our schematic calculations, although rigorous and complete sets of mode-coupling equations (and not an arbitrary phenomenological model) are considered. Consequently, it seems reasonable to us to assume that a schematic study of the molecular dynamics simulation results would reveal effective behaviors similar to those found for salol and CKN.

On the basis of the preceding discussion, we suggest a possible description of the approach of the calorimetric glass transition in term of effective temperature-dependent mode-coupling parameters. At high enough temperatures, the dynamics of a liquid are appropriately described by the ideal mode-coupling theory (in the sense that the dynamics are dominated by processes that couple the way the density correlators do in the MCT with vertices that are smooth functions of the static correlations in the system). When the temperature is lowered, the system seems to evolve toward the ergodic-to-non ergodic transition predicted by the theory. But, at a temperature notably higher than the extrapolated T_c , the dynamics depart from the predictions of the theory : it is better expressed in term of effective vertices

that are not directly related to the statics and behave such that the transition is avoided. Finally, at low temperature, a qualitative change in the nature of the relaxation processes reveals a possible underlying dynamical transition. Quantitatively, this picture exhibits two properties :

- the ideal mode-coupling approach leads to an overestimated ability of the liquids to freeze.
- incompatible values of the exponent parameters are determined : compared to the one calculated from the statics, the fitting of the scaling equation overestimates λ , whereas the effective behavior leads to an underestimation.

If this picture works well for CKN, this last point is not clear in the case of salol, where our schematic fits provide equal exponent parameters from the high temperature extrapolation and the scaling equation. It is thought to be a peculiarity of this system, when approached with our elementary model. In CKN, there is a relative equivalence between the contributions of the two correlators to the scattered intensity (the proportions are about 30%-70%), whereas in salol the second correlator represents about 95 % of the scattered intensity, as a consequence of the height of the α -peak much larger than the microscopic peak. Thus our calculations for salol reduce in reality in the GHz domain to a fit of this single correlator, that is in fact equivalent to a fit of the scaling equation in this domain (see figure 2). Only more complex models with more correlators could reveal the proposed picture.

The nature of the processes responsible for the transition to an effective mode-coupling behavior is of course of great interest. It is not clear that discrete processes as correlated jumps and hopping are good candidates, because in simulations they are generally characterized only well below the extrapolated critical temperature of MCT (for Lennard-Jones mixture,³⁴ $T_c = 0.922$ is predicted from statics, whereas the secondary peak of the self part of the van Hove correlation function generally associated to these processes appears below 0.5).

If the picture described here is valid, it introduces some questions about the relevance of the predictions of MCT in the vicinity of the dynamical critical transition, that we found to be widely avoided. It is thus necessary to know what is the maximum distance to the critical hypersurface at which the universal predictions of the theory are effective : schematic models can provide some answers to this determining problem.

First consider the elementary F_{12} -model for one density correlator defined by equations 4.1 and 4.2 alone. Following Götze and Sjögren,³⁶ we choose

$$v_1 = v_1^c (1 - \varepsilon) \quad v_2 = v_2^c (1 - \varepsilon) \quad (6.3)$$

such that $\lambda = 1/\sqrt{v_2^c}$ equals 0.7 on the transition line. ε is thus a kind of 'distance' from the transition line. After numerical integration and Fourier transform, the susceptibility spectra are fitted in the minimum region with the scaling equation (equation 3.10) in order to determine an effective exponent parameter λ_{eff} as a function of positive ε (figure 5). This procedure reproduces the usual way of treating experimental results beyond the scope of MCT. It is clear that for ε greater than 0.005, λ_{eff} departs notably from its value on the critical line and is never constant. It corresponds thus to a maximum distance from the transition line for the critical properties predicted by the theory to be effective.

In order to take into account this ε dependence, a vertices dependent exponent parameter can be defined following Götze and Sjögren.³⁷ In the case of the F_{12} -model and of our schematic model, which have exactly the same critical properties, this reads :

$$\lambda_{loc} = v_2 (1 - f)^3 \quad \text{with } f \text{ solution of } v_1 + 2 v_2 f = \frac{1}{(1 - f)^2} \quad (6.4)$$

valid only if

$$v_1 \geq 3 v_2^{2/3} - 2 v_2 \quad (6.5)$$

We see that, in the F_{12} -model, the introduction of local scaling equation parameters extends the domain of numerical compatibility of this equation to $\varepsilon = 0.015$, but it is not enough : effective parameters are determined out

of this range and even in the domain where the condition 6.5 is not obeyed. These results have thus no significance in term of the MCT and arise only because of the numerical flexibility of the fitting procedure.

The same problems should appear with the experimental spectra. Indeed the trajectories followed by salol and CKN in the parameters space of our model are not nearer, in term of a distance defined as ε is, from the transition line than are the points considered above. Moreover some experimental points do not obey the constraint 6.5.

We have performed scaling equation calculations as above for the susceptibility spectra of salol between 263 and 333 K. It is clear from figure 6 that the values of λ_{eff} vary notably with temperature and can be determined even when 6.5 is not valid. They are compatible with the previous determinations by other authors (table 1) but neither with λ_{vert} (table 4) nor with λ_{loc} coming from our schematic calculations.³⁷ This is representative of the ineffectivity of the reduction theorem, as is the existence of two distinct minima for each correlator at all temperatures (figure 7). Two possible reasons can be proposed for this, depending on the considered temperature domain. At high temperature, where the description of the dynamics by MCT is correct and alternative processes are not necessary, the supercooled liquid is too far from its transition point and thus the asymptotic predictions of the theory valid in the vicinity of the transition do not yet hold, whereas, at low temperature, processes that are not tractable within the mode-coupling formalism are probably at the origin of these discrepancies.

The point is thus that our simple schematic calculations indicate that the leading order critical predictions of the MCT are experimentally unobservable. The conclusion would have been the same even if there were no need of additional processes to describe the dynamics of the supercooled liquid in the transition region; it is found necessary the system to be very near its transition point, where error bars of mosts experimental techniques impose differences of several degrees to reveal significant evolutions. This necessity has been pointed out recently within the investigation of the next-to-leading

order corrections to the critical predictions of MCT,³ which are not for the moment available for experimental data like DLS spectra.

7 Conclusion

We have analyzed depolarized light scattering spectra of two fragile glass-forming liquids, salol and CKN, by means of schematic mode-coupling equations (*i.e.* a reduced closed set of non linear integrodifferential equations for correlation functions). Such simple models are interesting because they make possible tests of the MCT that are not limited to its asymptotic critical predictions. Moreover, they capture the essential structure of the mode-coupling equations with no reference to the details of the physical processes at work. It is thus possible to take into account in an effective manner processes that have not been included so far in the MCT. It is the case for instance of the orientational fluctuations.

We have found that the two-correlator model developed here gives a very good account of the experimental data. In particular, the so-called boson peak offers no extra-difficulty within our fitting procedure, whatever functional form is chosen for the memory kernel.^{4,5}

The evolution with temperature of the relaxational properties of the system can be rationalized in term of effective temperature-dependent mode-coupling vertices. It is compatible under certain assumptions with observations previously made in molecular dynamics simulations of simple liquids. Two temperature regimes can be introduced and interpreted as follow. At high temperature, the dynamics are well described by mode-coupling equations, in which the vertices are determined from the static correlations of the supercooled liquid. This regime corresponds in our fits to a linear evolution of the mode-coupling parameters with temperature. Approaching the MCT critical transition, the effective vertices depart from the linear behavior and exhibit an unexpected behavior : they follow the transition line without crossing it. The avoidance of the transition has been known for a long

time and is generally associated with the occurrence of so-called activated processes that are not included in the theory. However, in our picture, these competitive processes seem to be efficient well above the critical temperature predicted within the MCT formalism, in a domain where activated or hopping processes are not supposed to be important. An immediate consequence of this is that the universal, critical predictions of the theory should be unobservable experimentally.

That the MCT of the glass transition needs be completed is not a new idea, but it is *a priori* a difficult task. If the picture given here is valid, one would expect from a successful extension of MCT that it restores the quasi-linear variation of the effective vertices by introducing new ones that become important only at low temperature. In this respect, note that our results for the critical parameters extrapolated from high temperatures (where the necessary corrections to ideal MCT are thought to be of minor importance) do not allow to recover those from the so-called "extended mode-coupling theory" that has been proposed as an improvement of the ideal mode-coupling theory and was tested in its scaling form on salol and CKN.⁸

At last, it is necessary to point some remaining difficulties, that are of great interest but are out of the scope of this study. Of critical importance is the nature of the relaxation probed by the depolarized light scattering, density fluctuations or molecular reorientations.²² Fortunately, we find that the choice for the expression of the scattered intensity as a function of the schematic correlators has no influence on the results of fit. But it asks the question of the dynamics of molecular orientational processes in the super-cooled liquid phase and its role in the structural relaxation of molecular systems. Some evidence exists in simulations that this dynamics is the same as for density fluctuations and that the two processes are coupled.³⁸ The very good results of the schematic fits are also in favor of such a conclusion. Nevertheless, this remains to be demonstrated theoretically. Thus, in order to test the relevance of this approach from the experimental point of view, analysis of data from different spectroscopic techniques are necessary. With

this goal, coherent neutron scattering spectra (that probe directly the dynamic structure factor) and far infrared absorption data (that probe dipolar reorientations, thus molecular rotations) are now under study.

Acknowledgments

The authors are grateful to Prof. W. Götze for very helpful comments all along this work and Dr. M. Fuchs for providing them the codes for some parts of the calculations. We are also indebted to Prof. H.Z. Cummins and Dr. G. Li for the use of their experimental data on salol and CKN. We particularly acknowledge Dr. G. Tarjus for fruitful discussions and help in our understanding of the theory.

Note

After submission of this work, a paper was sent to us by W. Götze, which reports schematic calculations on DLS spectra of glycerol.³⁹ The model used in this paper and the results obtained will be discussed and compared to ours in further publication.²⁹

References

- [1] C.A. Angell, p.3 in *Relaxation in Complex Systems*, edited by K.L. Ngai and G.B. Wright (Office of Naval Research, Washington, 1984); C.A. Angell, J. Phys. Chem. Solids **49**, 863 (1988); C.A. Angell, in *Proceedings of the first Tohwa University International Symposium, Fukuoka, Japan, 1991*, AIP Conf. Proc. 256, edited by K. Kawasaki, T. Kawakatsu and M. Tokuyama (AIP, New York, 1992).
- [2] W. Götze, Philos. Mag. **43**, 219 (1981) ; E. Leutheusser, Phys. Rev. A **29**, 2765 (1984); W. Götze, p.287 in *Liquids, Freezing and Glass Transition (Les Houches, 1989)* , edited by J.P. Hansen, D. Levesque and J. Zinn-Justin (North-Holland, Amsterdam, 1991) and references therein; W. Götze and L. Sjögren, Rep. Prog. Phys. **55**, 241 (1992).
- [3] T. Franosch, M. Fuchs, W. Götze, M.R. Mayr and A.P. Singh, Phys. Rev. E, in print.
- [4] C. Alba-Simionesco and M. Krauzman, J. Chem. Phys. **102**, 15 (1995).
- [5] C. Alba-Simionesco, V. Krakoviack, M. Krauzman, P. Migliardo and F. Romain, J. Raman Spectroscopy **27**, 715 (1996).
- [6] V. Krakoviack, C. Alba-Simionesco and M. Krauzman, p.373 in *Non-equilibrium phenomena in supercooled fluids, glasses and amorphous materials, Pisa, Italy, 1995*, edited by M. Giordano, D. Leporini and M.P. Tosi (World Scientific, Singapore, 1996).
- [7] G. Li, W.M. Du, A. Sakai and H.Z. Cummins, Phys. Rev. A **46**, 3343 (1992).
- [8] H.Z. Cummins, W.M. Du, M. Fuchs, W. Götze, S. Hildebrand, A. Latz, G. Li and N.J. Tao, Phys. Rev. E **47**, 4223 (1993).
- [9] J. Toulouse, G. Coddens and R. Pattnaik, Physica A **201**, 305 (1993).

- [10] C. Dreyfus, M.J. Lebon, H.Z. Cummins, J. Toulouse, B. Bonello and R.M. Pick, Phys. Rev. Lett. **69**, 3666 (1992).
- [11] Y.W. Yang and K.A. Nelson, Phys. Rev. Lett. **74**, 4883 (1995); Y.W. Yang and K.A. Nelson, J. Chem. Phys. **103**, 7732 (1995).
- [12] G. Li, W.M. Du, X.K. Chen, H.Z. Cummins and N.J. Tao, Phys. Rev. A **45**, 3867 (1992).
- [13] F. Mezei, W. Knaak and B. Farago, Phys. Rev. Lett. **58**, 571 (1987); W. Knaak, F. Mezei and B. Farago, Europhys. Lett. **7**, 529 (1988); F. Mezei, J. Non-Cryst. Solids **131-133**, 317 (1991).
- [14] G. Li, W.M. Du, J. Hernandez and H.Z. Cummins, Phys. Rev. E **48**, 1192 (1993).
- [15] Y.W. Yang and K.A. Nelson, J. Chem. Phys. **104**, 5429 (1996).
- [16] P. Lunkenheimer, A. Pimenov and A. Loidl, submitted to Phys. Rev. Lett., 10/96.
- [17] W. Steffen, A. Patkowski, G. Meier and E.W. Fisher, J. Chem. Phys. **96**, 4171 (1992); W. Steffen, G. Meier, A. Patkowski and E.W. Fisher, Physica A **201**, 300 (1993); W. Steffen, A. Patkowski, H. Glaser, G. Meier and E.W. Fisher, Phys. Rev. E **49**, 2992 (1994).
- [18] A. Patkowski, W. Steffen, G. Meier and E.W. Fischer, J. of Non-cryst. Solids **172-174**, 52 (1994); W. Steffen, B. Zimmer, A. Patkowski, G. Meier and E.W. Fischer, J. of Non-cryst. Solids **172-174**, 37 (1994).
- [19] J. Jäckle, p.135 in *Amorphous solids : low-temperature properties*, edited by W.A. Phillips (Springer, Berlin, 1981).
- [20] V. Malinovski and A.P. Sokolov, Solid State Commun. **57**, 757 (1986); A.P. Sokolov, in *Dynamics of disordered materials II*, edited by A.J. Dianoux, W. Petry and D. Richter (North-Holland, 1993); U. Buchenau,

- Europhys. News **24**, 77 (1993); V.N. Novikov, E. Duval, A. Kisliuk and A.P. Sokolov, J. Chem. Phys. **102**, 4691 (1995).
- [21] E. Duval, N. Garcia, A. Boukenter and J. Serughetti, J. Chem. Phys. **99**, 2040 (1993); T. Achibat, A. Boukenter and E. Duval, J. Chem. Phys. **99**, 2046 (1993).
- [22] H.Z. Cummins, G. Li, W.M. Du, R.M. Pick and C. Dreyfus, Phys. Rev. E **53**, 896 (1996); erratum in Phys. Rev. E **55**, 1232 (1996).
- [23] S.P. Das and G.F. Mazenko, Phys. Rev. A **34**, 2265 (1986); B. Kim, Phys. Rev. A **46**, 1992 (1992); J. Yeo and G.F. Mazenko, Phys. Rev. E **51**, 5752 (1995).
- [24] T. Geszti, J. Phys. C **16**, 5805 (1983)
- [25] L. Sjögren, Phys. Rev. A **33**, 1254 (1986).
- [26] J. Bosse and U. Krieger, J. Phys. C : Solid State Phys. **19**, L609 (1986); U. Krieger and J. Bosse, Phys. Rev. Lett. **59**, 1601 (1987); U. Krieger and J. Bosse, Z. Phys. Chem. **156**, 97 (1988).
- [27] N.J. Tao, G. Li, X. Chen, W.M. Du and H.Z. Cummins, Phys. Rev. A **44**, 6665 (1991).
- [28] M.J. Stephen, Phys. Rev. **187**, 279 (1969).
- [29] V. Krakoviack, C. Alba-Simionesco, in preparation.
- [30] M. Fuchs, W. Götze, I. Hofacker and A. Latz, J. Phys. : Condens. Matter **3**, 5047 (1991).
- [31] P.J. Davis and P. Rabinowitz, in *Methods of Numerical Integration* (Academic press, New York, 1975).
- [32] W.H. Press, S.A. Teukolsky, W.T. Vetterling and B.P. Flannery, in *Numerical Recipes* (Cambridge university press, New York, 1985).

- [33] X.C. Zeng, D. Kivelson and G. Tarjus, Phys. Rev. E **50**, 1711 (1994);
P.K. Dixon, N. Menon and S.R. Nagel, Phys. rev. E **50**, 1717 (1994);
H.Z. Cummins and G. Li, Phys. Rev. E **50**, 1720 (1994).
- [34] W. Kob and H.C. Andersen, Phys. Rev. Lett. **73**, 1376 (1994); W. Kob
and H.C. Andersen, Phys. Rev. E **51**, 4626 (1995); W. Kob and H.C.
Andersen, Phys. Rev. E **52**, 4134 (1995); M. Nauroth and W. Kob,
Phys. Rev. E **55**, 657 (1997).
- [35] B. Bernu, J.P. Hansen, Y. Hiwatari and G. Pastore, Phys. Rev. A **36**,
4891 (1987); J.N. Roux, J.L. Barrat and J.P. Hansen, J. Phys. : Con-
dens. Matter **1**, 7171 (1989); J.L. Barrat and A. Latz, J. Phys. : Con-
dens. Matter **2**, 4289 (1990).
- [36] W. Götze and L. Sjögren, J. Phys. C : Solid State Phys. **21**, 3407 (1988).
- [37] W. Götze and L. Sjögren, J. Phys. : Condens. Matter **1**, 4183 (1989).
- [38] G.F. Signorini, J.L. Barrat and M.L. Klein, J. Chem. Phys. **92**, 1294
(1990).
- [39] T. Franosch, W. Götze, M.R. Mayr and A.P. Singh, Phys. Rev. E **55**,
3183 (1997).

Table 1: Parameters for MCT fits to salol data ($T_m = 315$ K, $T_g = 218$ K).

technique	T_c (K)	λ	references
DLS ^a , ideal MCT	256 ± 5	0.70	7
DLS ^a , extended MCT	250	0.73	8
neutron scattering	263 ± 7		9
Brillouin scattering	275 ± 10		10
viscosity	265 ± 5		7
ISLS ^b	266 ± 1		11

^adepolarized light scattering

^bimpulsive stimulated light scattering

Table 2: Parameters for MCT fits to CKN data ($T_m = 433$ K, $T_g = 333$ K).

technique	T_c (K)	λ	references
DLS ^a , ideal MCT	378 ± 5	0.81	12
DLS ^a , extended MCT	378	0.85	8
neutron scattering	368 ± 5		13
Brillouin scattering	375 ± 5		14
ISLS ^b	378 ± 2		15
Dielectric spectroscopy	375	0.76	16

^adepolarized light scattering

^bimpulsive stimulated light scattering

Table 3: Values of the temperature-independent parameters of the schematic model

	salol	CKN
$\Omega_0/2\pi$ (GHz)	1230	2000
Γ_0	0.11	0.3
$\Omega_1/2\pi$ (GHz)	160	900
Γ_1	5.2	2.6
r	37	10
γ	18.6	2.4

Table 4: Parameters from the schematic-model fits to salol and CKN data

	salol	CKN
T_c (K)	257 ± 5	388 ± 5
λ_{HT}	0.69 ± 0.02	0.73 ± 0.02
λ_{vert}	0.61 ± 0.02	0.69 ± 0.02

FIGURE CAPTIONS

Figure 1: Experimental depolarized light scattering spectra (for readability, some spectra are omitted and the data are reported every 2 points) and schematic fits. a) salol (the last two curves at 233 K and 253 K are obtained with a 90 GHz low frequency cut-off; the spectra at 243 K, 273 K, 293 K, 313 K and 333 K are omitted). b) CKN (the spectra at 383 K, 403 K, 423 K, 443 K and 468 K are omitted).

Figure 2: Individual contributions to the fitted DLS spectra of each of the two correlators of the schematic model in a semilogarithmic plot. a) salol at 333 K. b) CKN at 433 K. Note that the χ_0 contribution is negligible below 50 GHz for salol, but not for CKN. This explains the equivalence between a scaling-equation fit and our schematic calculations in the case of salol.

Figure 3: Vertices v_1 and v_2 of the schematic model as functions of temperature for salol and CKN. The straight lines correspond to the linear extrapolation described in the text.

Figure 4: Two-dimensional (v_1, v_2) parameter space of the schematic model and trajectories followed by salol and CKN with temperature.

Figure 5: Effective and local exponent parameters (resp. λ_{eff} and λ_{loc}) as functions of ε (see text for definition) for the one-correlator F_{12} -model.

Figure 6: Effective temperature-dependent, effective temperature-independent, and local exponent parameters (resp. λ_{eff} , λ_{global} , and λ_{loc}) as functions of temperature for supercooled salol above T_c .

Figure 7: Individual contributions to the fitted DLS spectra of each of the two correlators of the schematic model at the closest temperatures

higher than T_c (the scaling factor is such that the minima of susceptibilities are equal). a) salol at 263 K. b) CKN at 393 K. Note that the minima of both contributions (when they exist) occur at different frequencies, in disagreement with the asymptotic predictions of the mode-coupling theory.

FIGURE 1-a

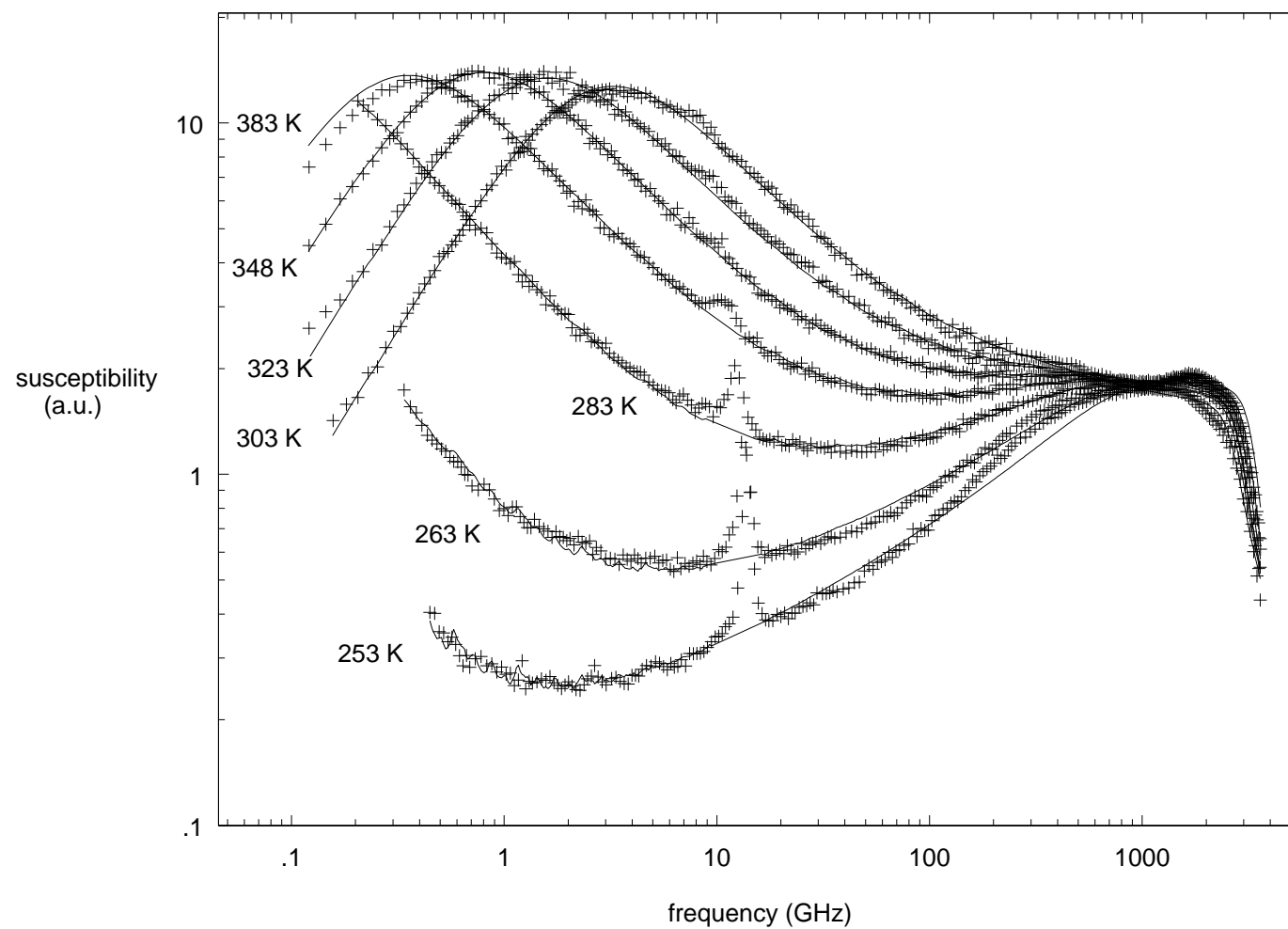


FIGURE 1-b

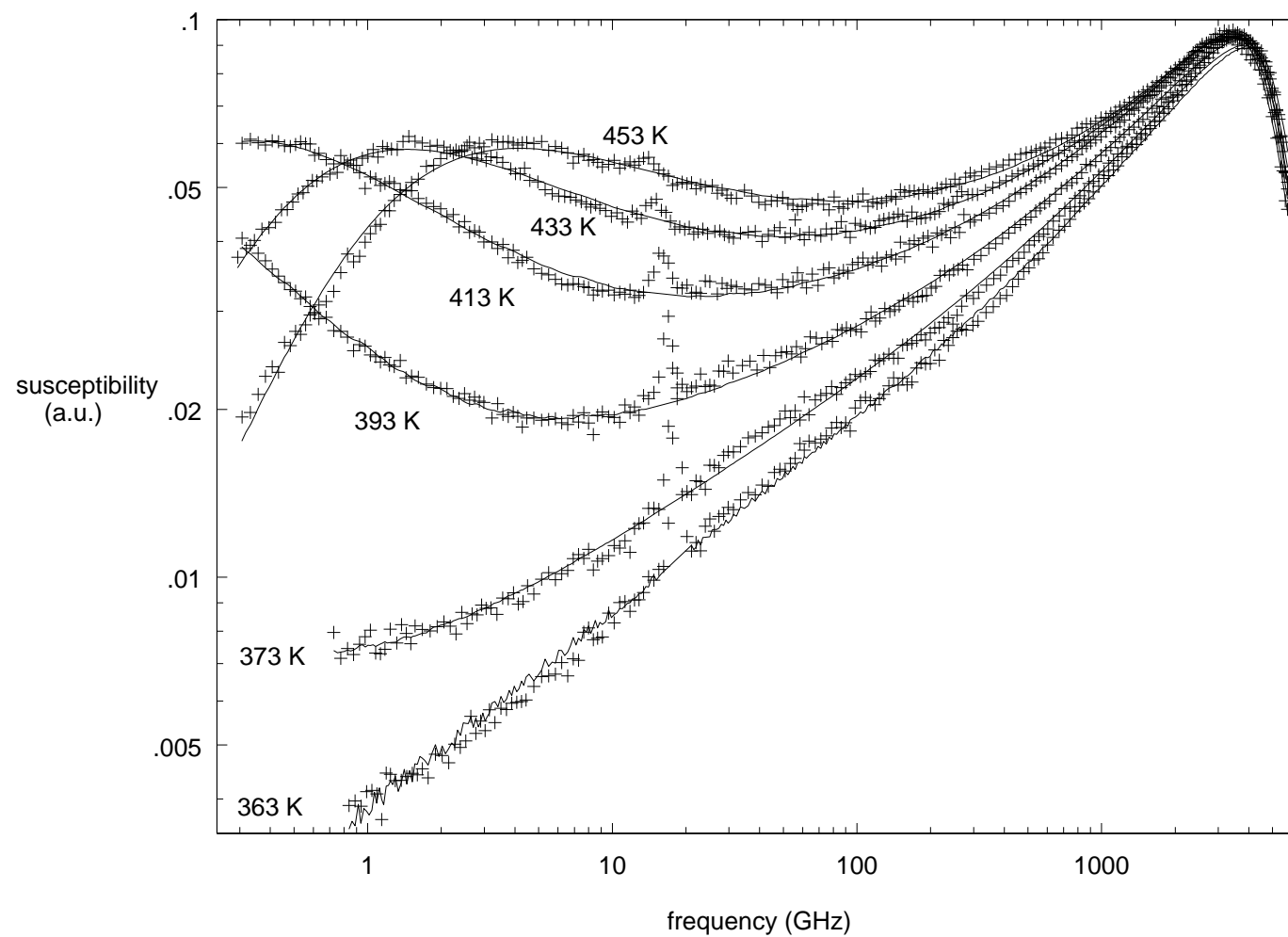


FIGURE 2-a

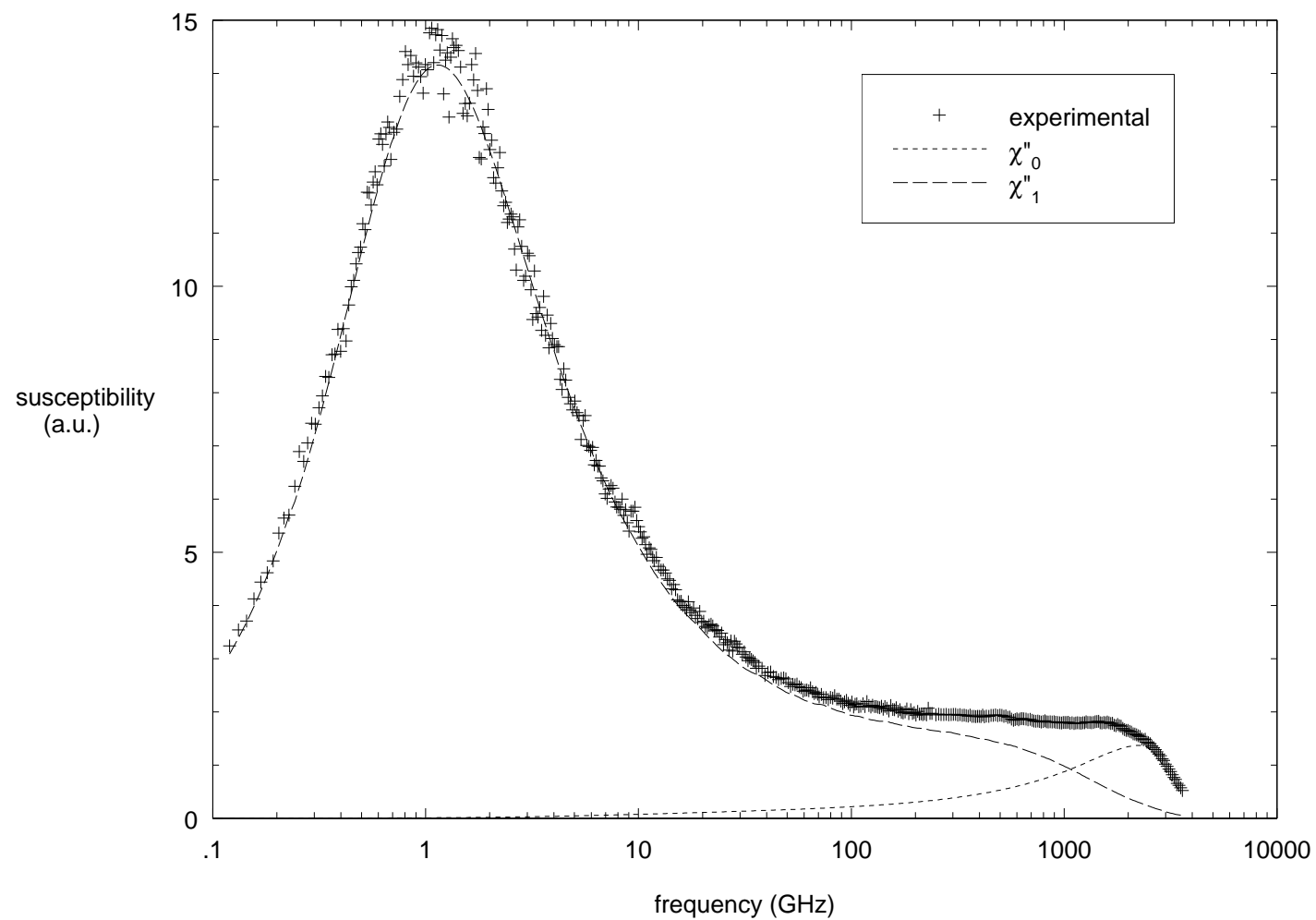


FIGURE 2-b

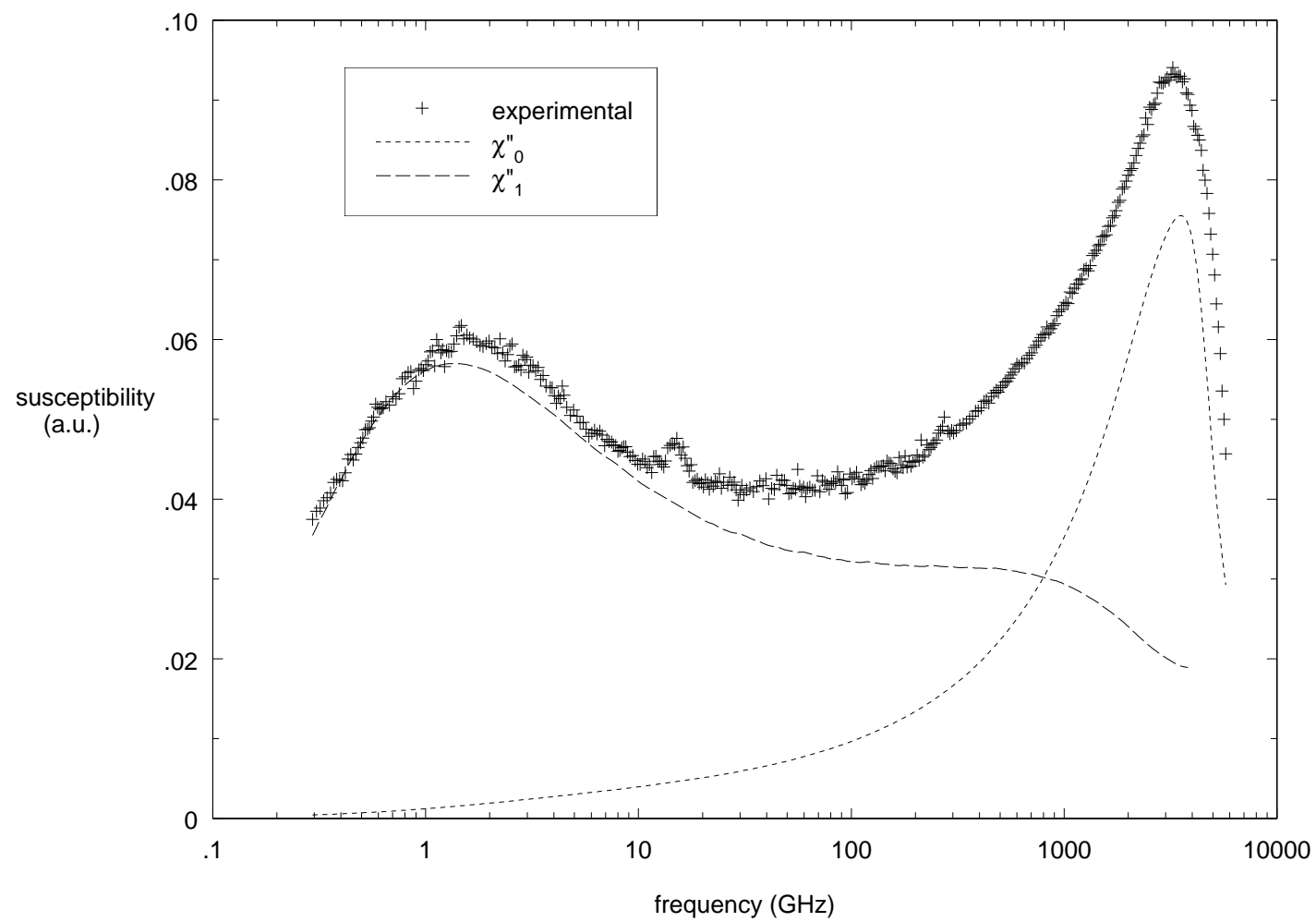


FIGURE 3

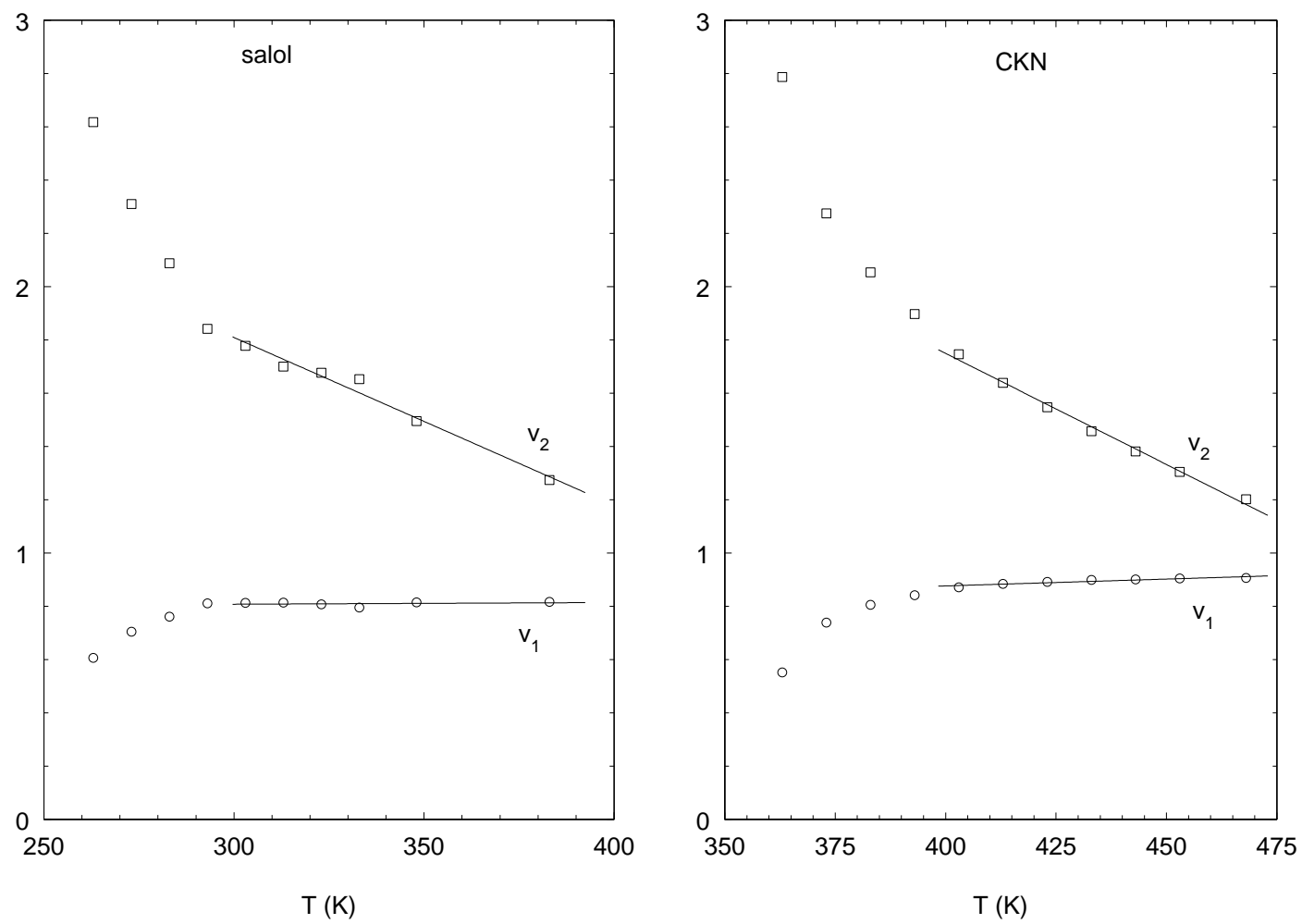


FIGURE 4

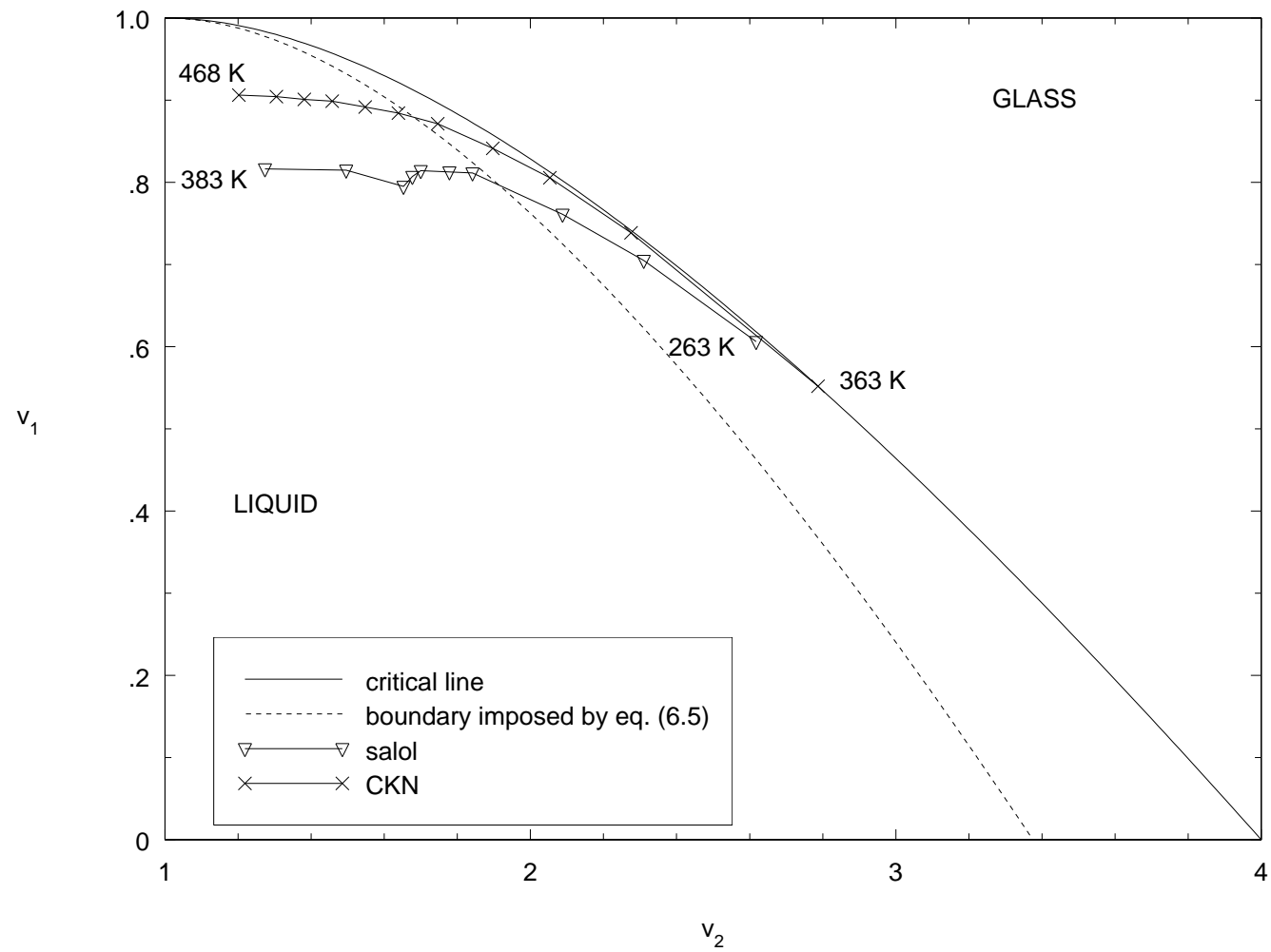


FIGURE 5

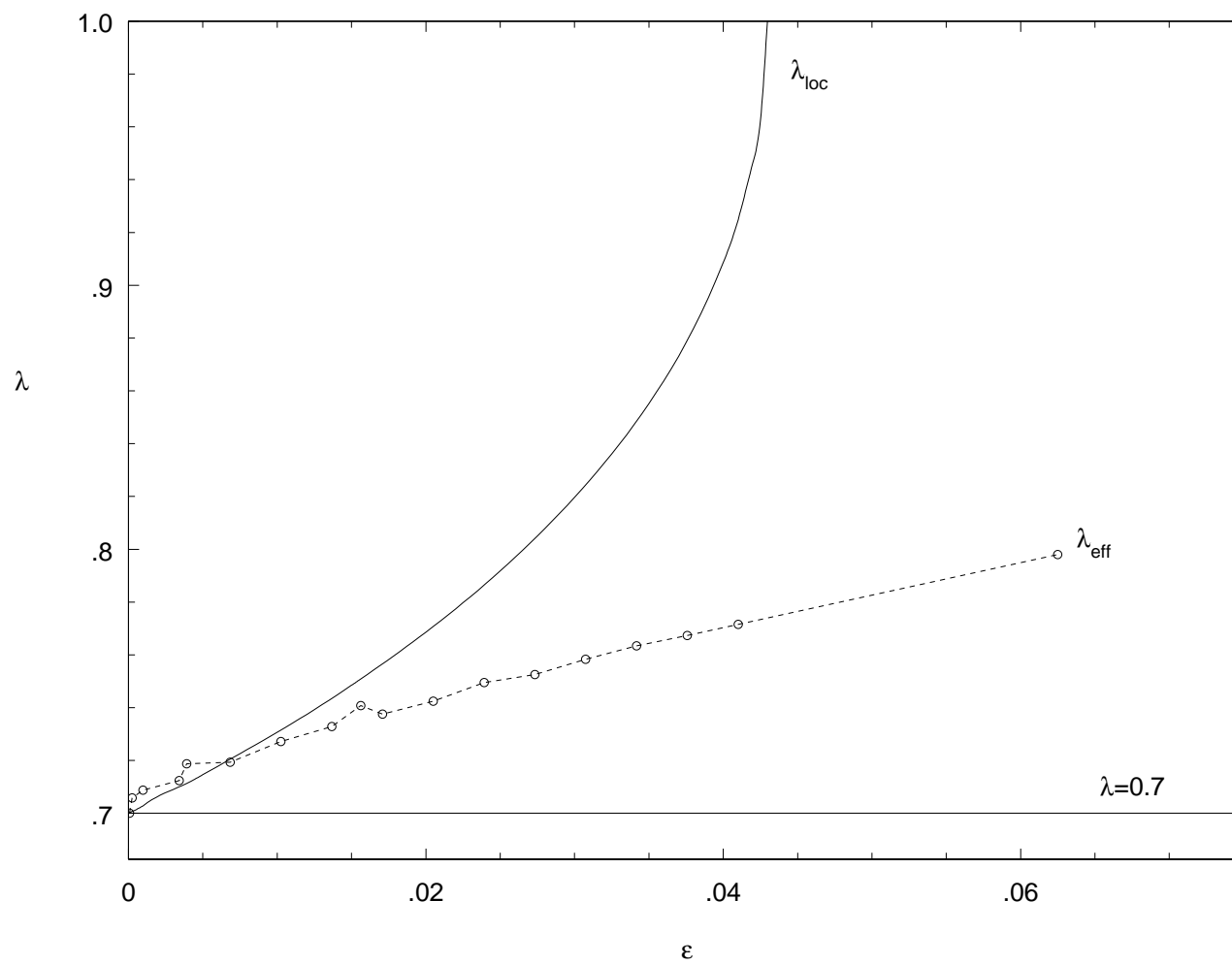


FIGURE 6

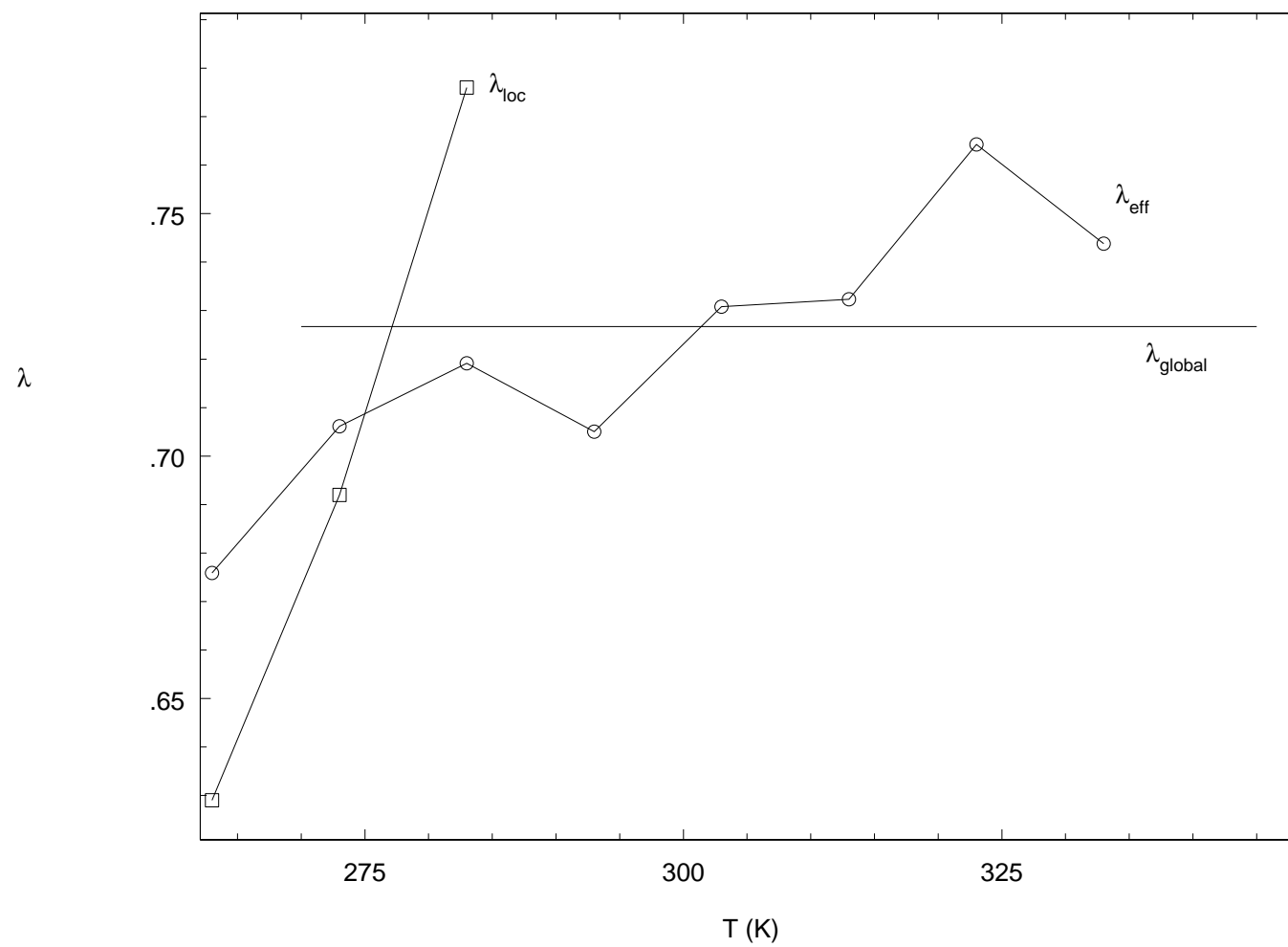


FIGURE 7-a

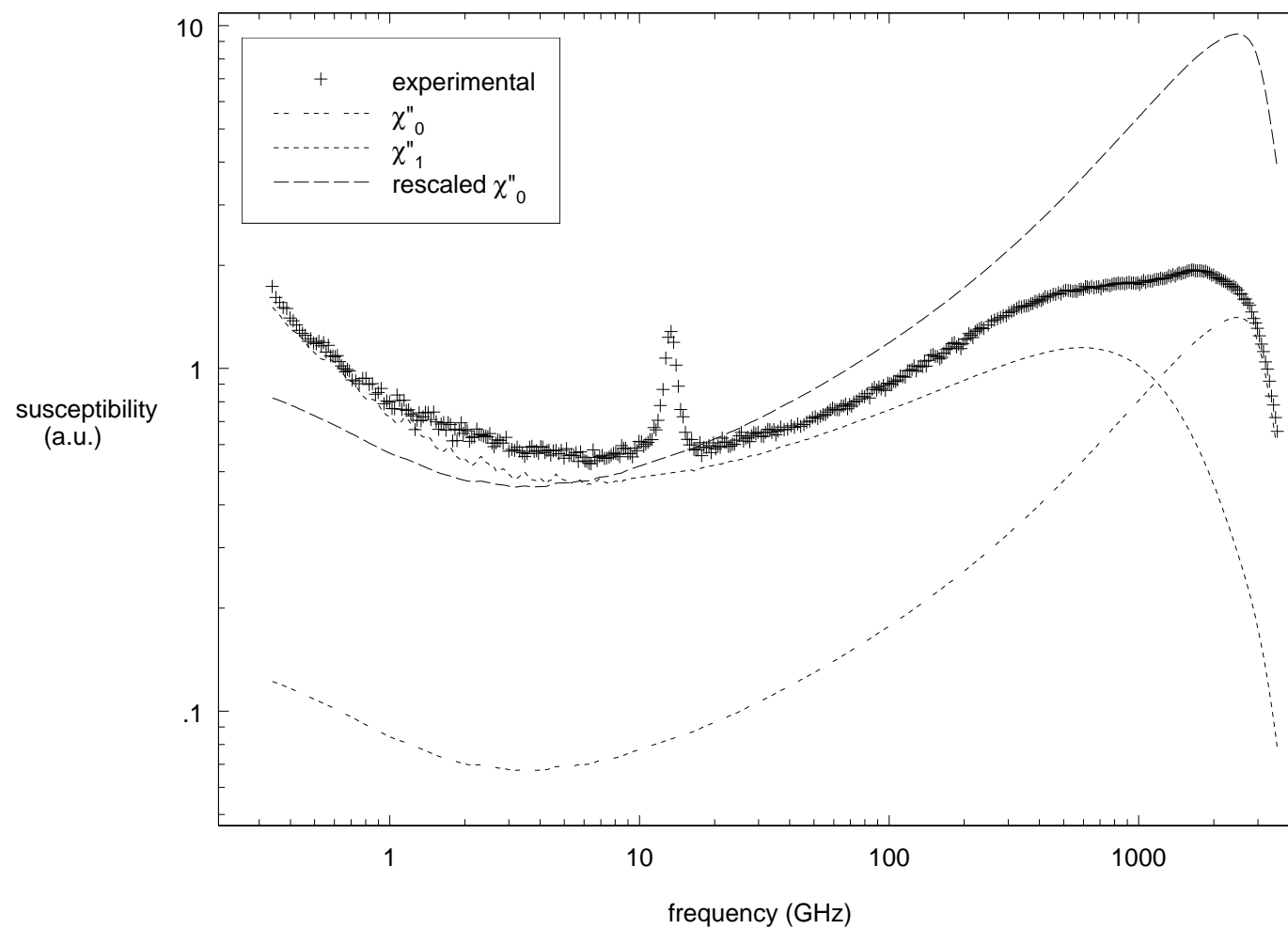


FIGURE 7-b

